



# Green instructions: Intelligent lighting via real-time chlorophyll fluorescence feedback: Enhancing yield and energy efficiency in controlled environment agriculture

Jim Stevens , Phillip Davey, Piotr Kasznicki, Tanja A Hofmann , Tracy Lawson <sup>\*</sup>

School of Life Sciences, University of Essex, Colchester CO4 3SQ, UK

## ARTICLE INFO

### Keywords:

Basil  
Chlorophyll fluorescence  
LEDs  
Plant communication  
Plant feedback system  
Photosynthetic efficiency  
Photosynthesis energy use  
Resource use  
Yield gain

## ABSTRACT

Controlled Environment Agriculture (CEA) delivers increased crop production per unit land, contributing to resilient food systems amidst challenges of climate change, population growth and urbanization. However, high energy costs and the associated carbon footprint for using LED lighting imposes substantial barriers to the widespread adoption of CEA. While light is indispensable for growth, critically its utilization by crops throughout the photoperiod remains sub-optimal, reducing photosynthetic efficiency and wasting energy. Here we have developed and demonstrated a novel real-time plant bio-feedback system that enables crops to directly 'communicate' optimal lighting requirements. Continuous non-invasive monitoring of photochemistry elicited decreased demand for light by basil at the end of the photoperiod, which, delivered by our system, improved yield per unit power. Specifically, our innovative approach increased yield by 13.5 % and reduced energy consumption per unit fresh mass by 6.2 %, delivering a 17 % decrease in CO<sub>2</sub> required to generate fresh mass yield. Application of this technique at scale can significantly improve resource management of CEA, supporting the productivity, profitability and sustainability of this food industry.

## 1. Introduction

Achieving sustainable increases in food production represents a significant political and social challenge, with key demographic drivers including the growing global population [1] and rising urbanization [2, 3]. Additionally, unpredictable weather patterns resulting from climate change add to those pressures [4]. As of 2020, agriculture itself contributes 14 % of global CO<sub>2e</sub> emissions [4], while yield gains are plateauing [5]; both issues need to be addressed urgently if global net zero targets and food security goals are to be realised.

Controlled Environment Agriculture (CEA) combines scientific knowledge with technological advancements to address these pressures on the sector [6]. CEA systems rely on cultivating crops within partially or entirely enclosed environments, which give growers a significant degree of control over growing conditions [7,8]. Horticulturalists are already able to reduce water, nutrient and pesticide inputs in CEA while increasing productivity [9], however, high electricity prices and the potentially high carbon footprint pressurise the viability of CEA where energy may represent up to 30 % of operating costs [10,11]. Yet the

industry holds great promise for the production of local, nutritious food while reducing transport costs and environmental impacts [12].

Vertical Farms are entirely closed, controlled environments where the grower must supply all inputs including light [13]. Increased cropping area per unit land in these systems can be coupled with year-round production capabilities [14] and those crops can be cultivated with enhanced nutritional value [15]. These factors fuel support for the VF industry, particularly in regions such as the Middle East and South-East Asia [6,16]. However, VFs are acutely sensitive to energy costs [13,17], making environmental sustainability and the capacity of the industry to achieve net zero questionable [18]. Nevertheless, CEA systems could lower CO<sub>2e</sub> emissions to the same level as broadacre agriculture by exploiting renewable energy sources [19], where possible. It has also been recognized that further environmental savings beyond exploring renewable energy are possible, most likely based on technological advancements [20]. Here we present a solution based on the design and development of a photo-feedback system that allows the crop to "communicate" directly with the LED growth lights, boosting productivity, reducing energy inputs and associated carbon footprint and thus

<sup>\*</sup> Corresponding author at: Department of Plant Biology & Institute for Genomic Biology, School of Integrative Biology, College of Liberal Arts and Sciences, University of Illinois at Urbana-Champaign; 1402 Inst for Genomic Biology, 1206 W Gregory Dr | M/C 195, Urbana, IL 61801.

E-mail addresses: [tlawson@essex.ac.uk](mailto:tlawson@essex.ac.uk), [tlawson3@illinois.edu](mailto:tlawson3@illinois.edu) (T. Lawson).

<https://doi.org/10.1016/j.atech.2025.101593>

Received 28 August 2025; Received in revised form 14 October 2025; Accepted 31 October 2025

Available online 1 November 2025

2772-3755/© 2025 The Authors. Published by Elsevier B.V. This is an open access article under the CC BY license (<http://creativecommons.org/licenses/by/4.0/>).

promoting sustainability.

Crop yields are determined by the accumulated rate of photosynthetic carbon uptake ( $A$ ) and are therefore correlated with light intensity and photoperiod. Currently the majority of indoor growth environments utilize square wave light regimes, which maintain light intensity at a constant level over the photoperiod [21–24]. Although there is correlation between light intensity and photosynthetic rate ( $A$ ), which drives crop growth [25–27], the efficiency at which light energy is utilised by plants is not always directly proportional to intensity, with a significant drop in  $A$  at high light intensities and towards the end of the photoperiod [28,29] (see Fig. 1). Under these circumstances, because lighting energy costs remain constant throughout the photoperiod, any decrease in  $A$  will lower crop light conversion efficiency [29]. Therefore, there is potential for substantial decrease in energy input by dynamically matching

the plants' light demand in real time [24,27].

Photosynthesis is determined by the rate of electron transport (ETR), in which the light energy absorbed by pigments drives the flow of electrons through photosystems I (PSI) and II (PSII) to produce ATP and reductant (NADPH), and by the rate of carbon fixation via Rubisco and the Calvin Benson cycle [30,31]. The absorbed light energy has one of three competing fates, it can be either: 1) utilised for these photosynthetic processes; 2) dissipated as heat (known as non-photochemical quenching (NPQ)); or 3) re-emitted at a longer wavelength known as chlorophyll fluorescence [30]. Measurements of chlorophyll fluorescence provide a rapid, scalable, non-invasive method to determine the efficiency of PSII photochemistry ( $Fq'/Fm'$ ), a proxy for  $A$  [30,32]. As light intensity increases, photosynthetic efficiency ( $Fq'/Fm'$ ) decreases, due to processes such as NPQ. Light intensities beyond saturation can

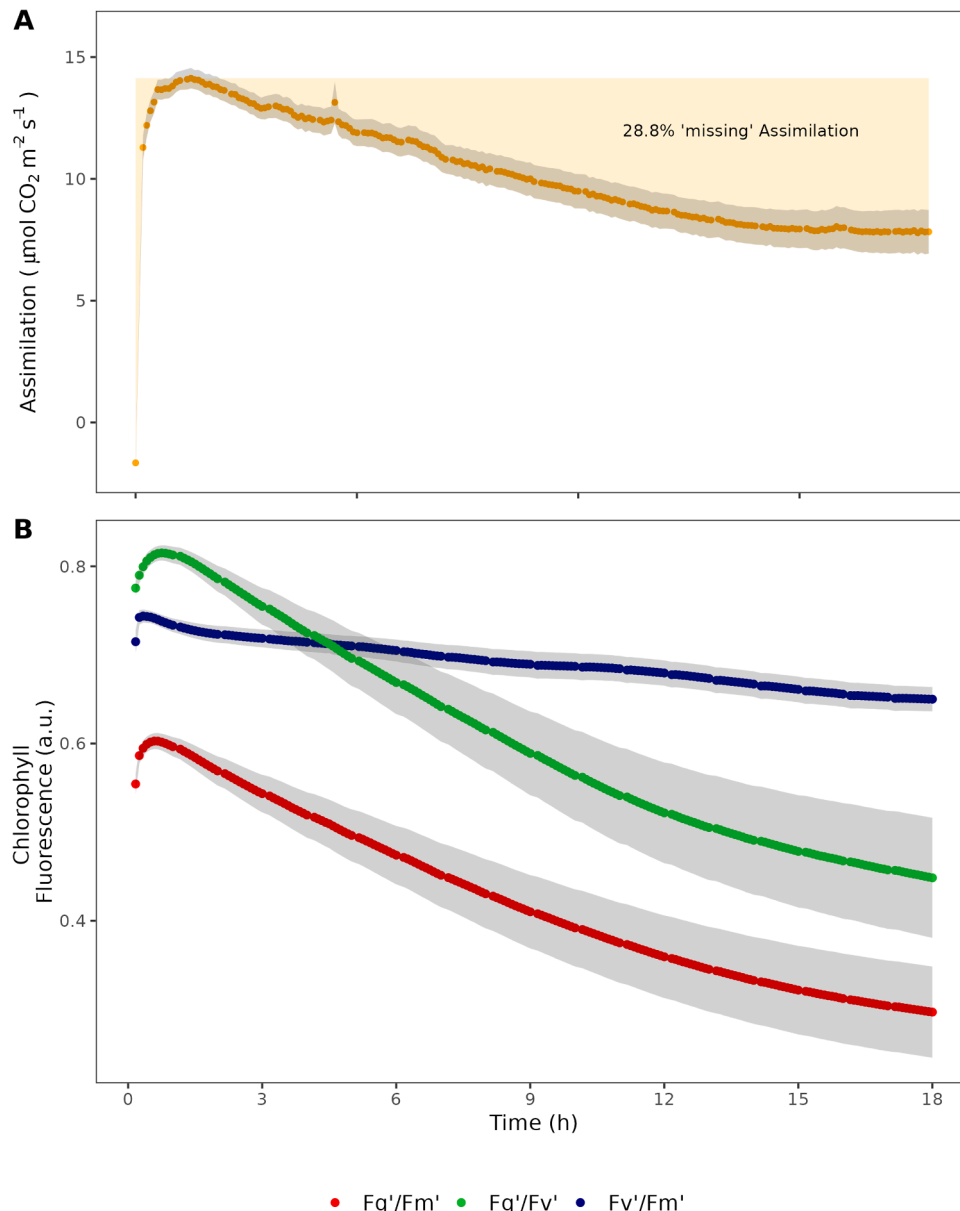


**Fig. 1. Diurnal measurements of assimilation rate and chlorophyll fluorescence parameters.** Basil (*O. basilicum* cv Sweet Genovese) plant responses to constant light conditions. Plants were exposed to  $400 \mu\text{mol m}^{-2} \text{ s}^{-1}$  PAR for 18 h at  $24^\circ \text{C}$ , 410 ppm  $\text{CO}_2$  & VPD 1.8 kPa. A) Photosynthetic  $\text{CO}_2$  assimilation ( $A$ ) showed a rise on exposure to light that continued for several hours to peak between 3 h and 6 h. Thereafter assimilation fell steadily for the remainder of the photoperiod. B)  $Fq'/Fm'$ , the operating efficiency of Photosystem II (PSII) is a function of  $Fq'/Fv'$  (the PSII efficiency factor) and  $Fv'/Fm'$  (maximal quantum efficiency of PSII). Changes in  $Fq'/Fm'$  were largely the result of changes in  $Fq'/Fv'$  implying that a falling efficiency factor drove the decrease in operating efficiency.  $Fv'/Fm'$  exhibited minimal change over the course of the measurement. Means shown  $\pm$  SE,  $n = 6$ . Area below the curve was integrated to calculate photosynthetic carbon gain over the diurnal period. This was compared to the maximum carbon gain if photosynthesis was maintained throughout the photoperiod.

result in damage to the PS's, known as photoinhibition, further decreasing  $Fq'/Fm'$  [30]. Additionally, factors other than light, such as temperature or nutrients, can also affect  $Fq'/Fm'$  and consequently, chlorophyll fluorescence is often employed to assess plant health in a broad spectrum of conditions [30,33,34].

Several studies in CEA have already shown that improving edible biomass of a number of indoor crops is possible by lowering light intensity over a longer photoperiod (compared to a higher intensity light for a shorter duration) [21,35–37]. Whilst this has improved lighting regimes in terms of plant growth and energy demand to some extent, it does not consider the aforementioned reduction in photosynthetic efficiency over the diurnal period. The integration of real-time measurements of chlorophyll fluorescence parameters, coupled with precision control of LED lighting systems, offers a technological advancement and exciting opportunity to adjust light based on the physiological responses of the plant [38–40], with great potential to improve sustainability.

Whilst Van Iersel et al. [41,42], developed a biofeedback system based on these principles and demonstrated that it was possible to maintain a wide range of ETRs and to distinguish between NPQ and photoinhibition to explain any reductions in photosynthetic efficiency, these studies provided proof of concept but did not assess the impact of such a feedback system on crop growth/yield and energy efficiency. By adjusting light intensity to match photosynthetic demand, we demonstrated a photo-feedback system that enhanced basil (*Ocimum basilicum*) yield while also reducing energy consumption. The result was a substantial improvement in cost effectiveness and sustainability of this CEA system. By dynamically adjusting LED intensity based on photosynthetic efficiency during the growing period, we highlight the considerable potential in biofeedback systems.

## 2. Methods

### 2.1. Plant growth conditions

Seeds of *Ocimum basilicum* (sweet basil) (Suttons Seeds, Paignton, UK), were sown in 0.29 dm<sup>3</sup> plastic pots containing compost (F2S, ICL Agriculture Ltd, UK). Pots were placed directly into the controlled environment growth chamber (Fitaclima PLH, Aralabs SA, Albarraque, Portugal), under 300  $\mu\text{mol m}^{-2} \text{s}^{-1}$  Photon Flux Density (PFD) at pot height, provided by LED growth lights (Dyna, Heliospectra AB, Gothenburg, Sweden). Photoperiod was 16 h, with an air temperature of 23 °C and a vapour pressure deficit (VPD) of 1.0 ( $\pm 0.2$ ) kPa. At 10 d post germination, plants were thinned to leave one individual per pot. At 14 days post germination, 24 plants were selected at random, split into control and treatments groups, and moved to a second growth environment, comprising of two independent lighting regimes. The first 'controlled' regime, consisted of a constant light intensity of 385  $\mu\text{mol m}^{-2} \text{s}^{-1}$  at the top of the crop canopy for a 18 h photoperiod. The intensity was selected to represent general LED lighting used in vertical farms, based on our assessment of commercially available luminaires and published data for leafy greens [43]. Air temperature and VPD were controlled to 22.1 °C ( $\pm 0.9$  °C) by day / 22.0 °C ( $\pm 0.5$  °C) by night and 1.07 ( $\pm 0.2$ ) kPa by day / 0.8 ( $\pm 0.1$ ) kPa by night respectively. In the second or 'feedback' regime, light intensity was dependent on feedback generated by a control loop based on the photophysiology of the crop.

### 2.2. Preliminary study

Previous studies have highlighted a decline of photosynthesis under constant light intensity [28]. To confirm the photosynthetic response of basil to constant (square) wave light, photosynthetic gas exchange with parallel chlorophyll fluorescence was measured every 5 min over an 18 h photoperiod (Li6800, Licor, Lincoln, Nebraska, US). Measurements were made on the youngest, fully expanded leaves in eight basil plants 20 d after germination (Fig. 1).

### 2.3. Control loop setup

A chlorophyll fluorimeter (PSP, ADC BioScientific, Hoddesdon, Herts, UK) measured the quantum efficiency of Photosystem II ( $Fq'/Fm'$ ) every 5 min and maximum quantum efficiency ( $Fv/Fm$ ) every 15 min during the day and night respectively. These measurements were made on the youngest fully expanded leaf of the crop at a constant distance (270 mm) from the growth light (Fig. 2). The fluorescence ratio  $Fq'/Fm'$  measured by the fluorimeter was output as an analogue (0 to 5 v) signal and passed to an Arduino microprocessor (Uno, Arduino, Italy). A Proportional Integral (PI) feedback loop was used to compare the measured fluorescence against a setpoint intended to generate constant photosynthetic efficiency. The PI controller aimed to minimise the error term  $e_t$  in the functions:

$$e_t = r_t - y_t$$

Where  $e_t$  was the error term at time  $t$ , expressed as the difference between the setpoint  $r_t$  (the desired value for  $Fq'/Fm'$ ) and the measured value of  $Fq'/Fm'$ ,  $y_t$  at that time. Having established  $e_t$ ,  $u_t$  was calculated:

$$u_t = K_p e_t + K_i \int_0^t e_t d\tau$$

Where  $u_t$  is the new setting for the luminaire (Dyna, Heliospectra, Sweden). The constants  $K_p$  and  $K_i$  were the multipliers for the proportional and integral elements of the control loop respectively and  $e_t$  represented the errors accumulated from time  $t_0$  to present.  $K_p$  and  $K_i$  were empirically determined from observation of system performance, with values of 350 and 50 respectively selected to ensure convergence towards the setpoint (Supplementary data, dotted line) without excessive noise (e.g. Supplementary Fig. 1, panel  $K_p = '1000'$ ). No derivative was used in the process control as overshoot in the system was limited. As a result, the control loop was able to adjust light intensity in response to changes in plant photosynthetic efficiency as measured by chlorophyll fluorescence parameter,  $Fq'/Fm'$ . The error between measured and setpoint values was used to calculate the output  $u_t$  which was then fed forward as a new setting for the luminaire. The setpoint of 0.52 was empirically determined (Fig. 2) to deliver a system that was both responsive and stable, was close to the inflection point of the photosynthetic light response curve (Fig. 3A) and to the midpoint of the fluorescence response curve (Fig. 3B). It was important to prevent large accumulation of errors in the integral term given the maximum and minimum light settings, which would severely affect system sensitivity. Consequently, integral wind-up was limited to the value reached when either Proportion < 0 and Integral < 0 and  $u_t = 18$  (i.e. at 100  $\mu\text{mol m}^{-2} \text{s}^{-1}$ ) or Proportion > 0 and Integral > 0 and  $u_t = 83$  (i.e. at 450  $\mu\text{mol m}^{-2} \text{s}^{-1}$ ).

All channels (representing different peak wavelength outputs of the LEDs) were given the same numeric setting in the luminaire software (Heliospectra), however light intensity outputs in each channel varied due to differences in LED efficiency. The Arduino was connected to a laptop that ran a Python script communicating with the luminaire over a direct ethernet connection (Fig. 2). In order to determine the target  $Fq'/Fm'$  setpoint, photosynthetic CO<sub>2</sub> uptake in parallel with measurements of  $Fq'/Fm'$  as a function of light intensity were made using an infra-red gas analyser with an integral chlorophyll fluorimeter (Li6800, LiCor Inc., Lincoln, Nebraska, USA). Measurements were made at a leaf temperature of 23 °C, VPD of 1.1 ( $\pm 0.1$ ) kPa. Photosynthesis was allowed to reach a steady state rate at 1300  $\mu\text{mol m}^{-2} \text{s}^{-1}$  and reduced stepwise to 1100, 900, 700, 550, 400, 250, 150, 100, 50 and 0  $\mu\text{mol m}^{-2} \text{s}^{-1}$ .

### 2.4. Experimental procedure

Every 24 h before the start of the photoperiod, plants were re-randomised within light treatments. Tray height was adjusted to

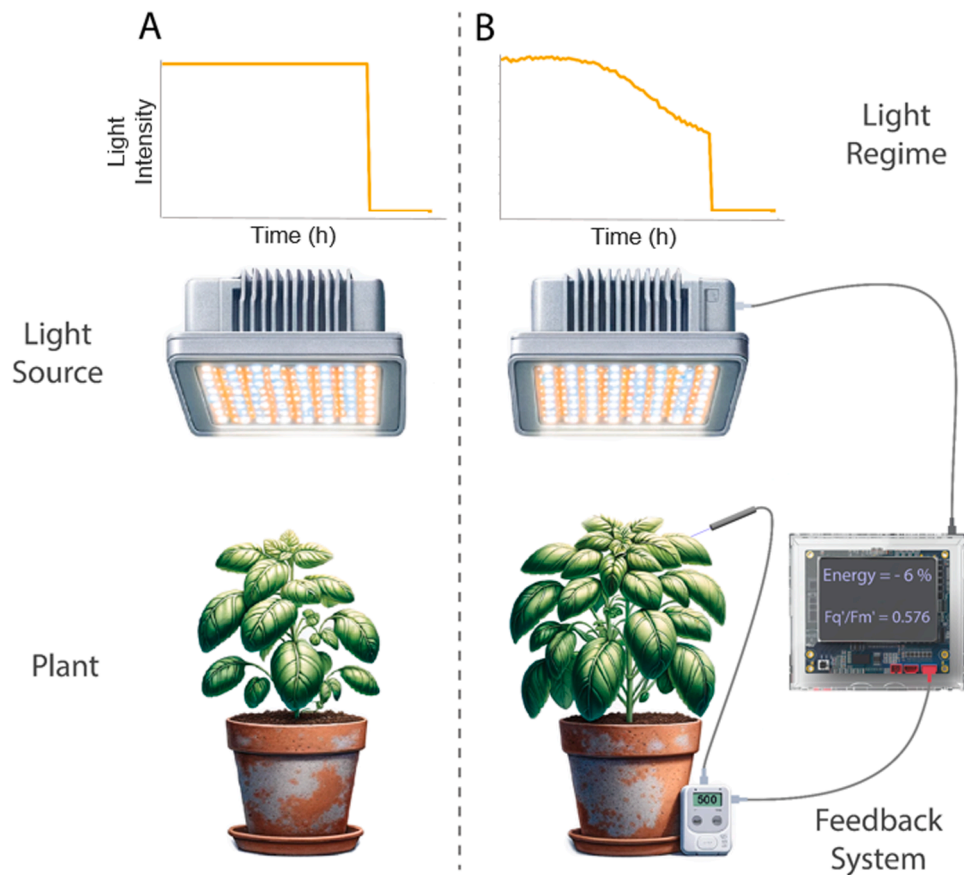


**Fig. 2. Schematic diagram of the experimental setup.** After seedling stage, basil plants were placed in one of two growth conditions for the duration of the experiment as soon as the youngest fully expanded leaves were large enough to be measured effectively. A) In the 'Controlled' treatment, plants were illuminated in a temperature-controlled environment of 23 °C for 18 h in 24 h at  $385 \mu\text{mol m}^{-2} \text{s}^{-1}$ . B) In the 'Feedback' treatment, plants were probed using an optisciences PSP32 Chlorophyll Fluorescence probe and datalogger. Variance in  $F_q'/F_m'$  compared to an empirically-defined setpoint of 0.52 was passed through a Proportion-Integration control loop and corrective intensity of illumination applied by a connection to a Heliospectra Dyna LED luminaire in a closed loop. Illumination in the feedback system was limited to a maximum of  $450 \mu\text{mol m}^{-2} \text{s}^{-1}$  and a minimum of  $100 \mu\text{mol m}^{-2} \text{s}^{-1}$ . Day length was identical to the control at 18 h.

maintain a constant distance from the lamp to the top of the canopy, controlling for the risk of plant height systematically influencing total light capture.

Measurements of  $F_q'/F_m'$  were taken on a youngest fully-expanded leaf at the top of the canopy from a plant that was changed randomly every day. Daily changes in the measured leaf allowed us to take into account the natural variation that exists between and within plants. The crop was watered daily with equal quantities of water for each treatment, with an addition of nutrients at 21 d post germination. The power consumption for each lamp was recorded using a power meter (MP001186, MultiComp, London, UK).

After 28 d growth, leaf area, fresh and dry mass were assessed for each individual plant. Leaf area was determined using a leaf area meter (LI-3100C, Li-Cor Inc.). Above ground biomass (leaves and stems) were dried to constant mass at 60 °C, and total dry mass measured using a 1 mg resolution balance (2006 MP, Sartorius, Germany). Six independent trials were conducted to evaluate the operation of the feedback system with suitable differences in the surrounding environmental conditions (Suppl. Table 1).

To establish the importance of the results observed on yield and energy use, effect sizes were calculated for all variables.

### 2.5. Data collection and statistical analysis

Data were analysed using R statistical software in the RStudio online application [44,45] (r Core Team 2021; Rstudio 2020). Linear models were attempted, with residuals tested for normality and

heteroskedasticity. For biomass and power-related data, linear mixed-effect models were used [46], with trial number considered a random effect to account for the variability in the growth environment and uncertainty over the size of the plants at the start of each trial. The mixed-effect models were compared to equivalent linear models in ANOVAs to check for best fit using the Akaike Information Criterion. Treatment effects within the mixed-effect models were also tested as ANOVAs [47]. Effect sizes for biomass and power parameters were calculated as Cohen's *d* measure [48].

### 3. Results

Our diurnal measurements of CO<sub>2</sub> assimilation and photosynthetic efficiency in basil grown under conventional square-wave lighting regimes supported observations in other species [29,49,50], that photosynthetic parameters decreased later in the photoperiod (Fig. 1). Photosynthesis increased to a maximum of approximately  $14 \mu\text{mol m}^{-2} \text{s}^{-1}$  during the initial 6 h of the photoperiod, after which there was a steady decrease in *A* to approximately  $10 \mu\text{mol m}^{-2} \text{s}^{-1}$  by the end of the 18 h photoperiod (Fig. 1). If the maximum photosynthetic rate observed post-dawn had remained constant throughout the 18 h photoperiod, an additional 254 mmol m<sup>-2</sup> CO<sub>2</sub> could have been assimilated, representing a 28.8 % loss of potential *A* over this period.

Photosynthetic efficiency ( $F_q'/F_m'$ ) decreased from 0.603 at the start of the photoperiod to 0.294 at the end of the photoperiod, which was mirrored by a decrease in  $F_q'/F_v'$ , which declined from 0.815 to 0.591 during the photoperiod. The maximum photosynthetic efficiency in the



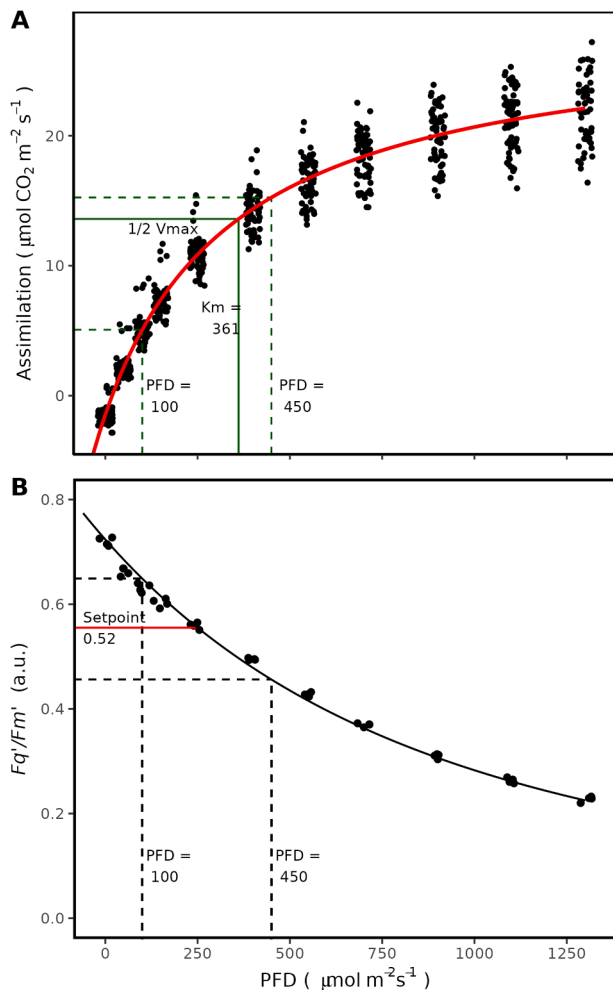


**Fig. 3. Light response curves of photosynthetic carbon assimilation and photosynthetic efficiency.** Selection of feedback parameters for the operation of the 'Green Instructions' chlorophyll fluorescence device was an empirical process. A). Photosynthetic CO<sub>2</sub> assimilation (A) as a function of light intensity (black points) was modelled as a Michaelis-Menten enzyme kinetic (red line). The inflection point  $1/2 V_{\text{max}}$ , where the plants were most sensitive to a change in light intensity, was observed at a value  $K_m = 361 \mu\text{mol m}^{-2} \text{ s}^{-1}$  PPFD.  $K_m$  lay between the minimum and maximum selected values of  $100 \mu\text{mol m}^{-2} \text{ s}^{-1}$  and  $450 \mu\text{mol m}^{-2} \text{ s}^{-1}$  which represent the economically viable range of intensities used by growers and incorporates both first and zeroth order segments of the curve.  $n = 20$ . B). The response of the operating efficiency of photosystem II as a function of PFD was modelled as a Gompertz function. The position of the empirically determined setpoint of  $F_q'/F_m'$  at 0.52 lay at approximately the midpoint of  $F_q'/F_m'$  observed at the maximum and minimum light intensity settings.  $n = 6$ .

light ( $F_v'/F_m'$ ) remained broadly unaltered, ranging between 0.603 and 0.412 through the photoperiod (Fig. 1B). These data demonstrated the close coupling between A and  $F_q'/F_m'$ , which our feedback system is based on.

The set points for input into the feedback system were determined by assessing A and  $F_q'/F_m'$  as a function of light intensity (Fig. 3). As expected, A increased with PFD reaching a maximum value of  $20.8 \mu\text{mol m}^{-2} \text{ s}^{-1}$  at  $1300 \mu\text{mol m}^{-2} \text{ s}^{-1}$  PFD. The operating efficiency of PSII photochemistry  $F_q'/F_m'$  decreased with increasing light intensities, with the lowest values of 0.23 observed at  $1300 \mu\text{mol m}^{-2} \text{ s}^{-1}$  PFD. The upper limit of light intensity for the feedback system was set at  $450 \mu\text{mol m}^{-2} \text{ s}^{-1}$ , above the inflection point ( $K_m$ ) for the PFD response curve. The upper limit was selected to: a. Allow the system to capture zeroth order (high light intensity) kinetics of the photosynthetic system and b. Represent a level achievable for a commercial grower's lighting systems.

The minimum intensity of  $100 \mu\text{mol m}^{-2} \text{ s}^{-1}$  was selected as it was above the light compensation point (where A crosses the x-axis in Fig. 3A) for basil. It also represented a minimal level of light intensity easily achievable and often used in commercial CEA systems and captured the first-order kinetics (low light intensity) of the modelled Michaelis-Menten curve. The specific  $F_q'/F_m'$  setpoint of 0.52 for the feedback system was determined from the mid-point value between the light intensity range described above (Fig. 3B). Crucially, this represented the highest photosynthetic rate whilst still maintaining a high quantum efficiency (mols carbon assimilated per mol photons supplied). For a  $F_q'/F_m'$  value  $>0.52$ ,  $e_t$  was negative (i.e. plant photosynthetic efficiency was too low), and the system tended to decrease light intensity, whereas, for a value  $<0.52$ ,  $e_t$  was positive and light intensity tended to increase.

Using the photo-feedback system both fresh and dry biomass and leaf area were significantly higher ( $p < 0.01$ ,  $p < 0.05$  and  $p < 0.001$  respectively, Fig. 4A–C) than in plants grown under square wave light regimes. Harvestable fresh mass, a critical determinant of retail value, increased by 13.5 %, equating to 0.9 g per plant. Similarly, leaf area increased by  $34.5 \text{ cm}^2$  per plant, an improvement of 17.7 %.

Importantly these higher yields were achieved at a significantly lower total energy demand for lighting ( $p < 0.05$ , Fig. 5A). This difference equated to a mean saving of 1.55 kWh or 6.19 % over the growth period (Fig. 5A). As a result, this significantly increased mean fresh mass, dry mass and leaf area *per unit energy consumed* (Fig. 5B–D;  $p < 0.01$ ,  $p < 0.01$  and  $p < 0.001$  respectively). The commercially important metric of fresh mass yield per unit power increased by 17.3 %, improving yield by over 0.05 g per plant for every kWh consumed. Moreover, the photo-feedback system increased foliar area by  $1.96 \text{ cm}^2 \text{ kWh}^{-1}$  or 25.0 % per plant. To establish the source of the observed increase in fresh and dry mass treatment effects (Figs. 4 & 5), we tested the relative water content (RWC) and specific leaf area (SLA). There were no differences between control and feedback conditions in RWC (Fig. 6A,  $p = 0.71$ ) or in SLA (Fig. 6B,  $p = 0.24$ ).

The photo-feedback system achieved gains in yield and savings in energy input by optimising light intensity over the diurnal period tuned to photosynthetic demand. During the first 9 h of the photoperiod, a significantly higher photosynthetic 'demand' (e.g. at 3 h,  $p < 0.01$ ) resulted in light intensity being controlled to approximately  $420 \mu\text{mol m}^{-2} \text{ s}^{-1}$ , close to the maximum intensity of  $450 \mu\text{mol m}^{-2} \text{ s}^{-1}$  in the photo-feedback system. Following this period, light requirement decreased steadily and from approximately 10 h into the photoperiod, was consistently below the light intensity in the control. For example, at 15 h, light intensity dropped to  $260 \mu\text{mol m}^{-2} \text{ s}^{-1}$ , 32 % below and significantly different to the  $385 \mu\text{mol m}^{-2} \text{ s}^{-1}$  fixed intensity for the 'Controlled' light regime ( $p < 0.001$ ) (Fig. 7A). Over the entire photoperiod, the gradual decline in PFD demand in the feedback system resulted in a lower mean intensity of  $342 \mu\text{mol m}^{-2} \text{ s}^{-1}$  (Fig. 7), compared to  $385 \mu\text{mol m}^{-2} \text{ s}^{-1}$  in the control. There were no differences in  $F_q'/F_m'$  during the initial 8 h between the control and photo-feedback system (Fig. 7B). In both treatments,  $F_q'/F_m'$  was approximately 0.63 at the start of the photoperiod, decreasing steadily in parallel to approximately 0.55 at 8 h. After 8 h the photo-feedback and control  $F_q'/F_m'$  values diverged. In the photo-feedback system, light intensity decreased (see Fig. 7A) to maintain  $F_q'/F_m'$  around the target of 0.52. This adjustment prevented the steep decline in operating efficiency seen in the control after 9 h (Fig. 7B), where at 15 h into the photoperiod,  $F_q'/F_m'$  in the control was 0.47 compared to 0.52 in the feedback system, which represented a substantial decline. Interestingly, while there was a  $39.0 \mu\text{mol m}^{-2} \text{ s}^{-1}$  difference in light intensity between control and feedback at the start of the photoperiod (e.g. 3 h after 'dawn'), this was not reflected in differences in  $F_q'/F_m'$ . Cumulatively, the photo-feedback condition consistently consumed less energy than the control condition (Fig. 7C).

To explore the underlying drivers of the observed differences in  $F_q'/F_m'$  further, the data were broken down into the two following components that determine the operating efficiency [30] PSII efficiency

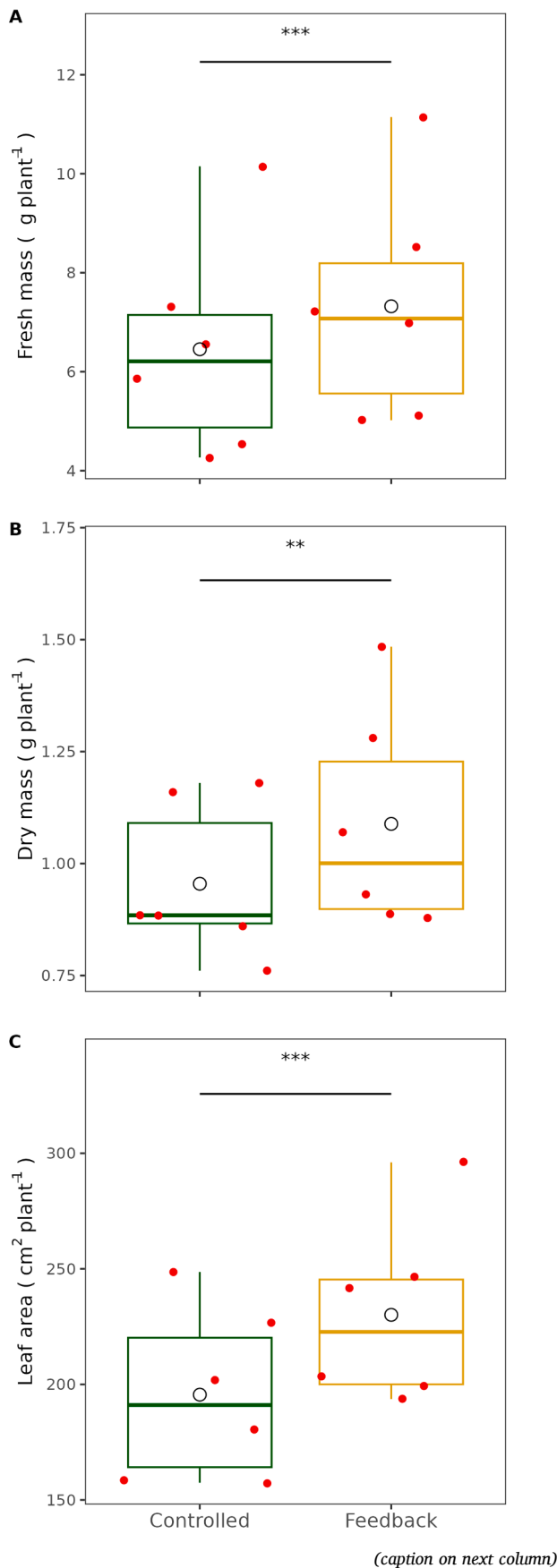


**Fig. 4. Harvest data from control and feedback grown plants.** The harvest results of the feedback system consistently outperformed the controlled-lighting system. Data were analysed using a linear mixed effects model of the form  $\text{lme}(\text{Harvest} \sim \text{Treatment} + (1|\text{Experiment\_number}))$ . This approach captured more of the uncertainty in the (semi-controlled) environmental conditions experienced compared to a traditional linear model. Aikike Information Criteria were consistent for all results, with the mixed-effects model outperforming the linear model. A) Fresh mass of above-ground basil plants were significantly higher in the Feedback condition, B) Dry mass of above-ground basil plants were also significantly higher in the Feedback condition, C) Meanwhile, mean leaf area of basil plants were significantly higher in the Feedback condition. Red points represent the means of 12 technical replicates for each independent trial, and the black circle is the overall mean for each treatment,  $n = 6$ . Significance levels: \*\*\* = 0.001, \*\* = 0.01, \* = 0.05.

factor ( $Fq'/Fv'$ ), which is non-linearly related to the proportion of PSII centers that are open, and the maximal quantum efficiency at the prevailing light intensity,  $Fv'/Fm'$  (Fig. 8) (Murchie & Lawson, 2013). Initially  $Fq'/Fv'$  was at the same level for both controlled and photo-feedback grown plants. However, after 8 h into the lighting period, the decrease in  $Fq'/Fv'$  was reduced in the control compared with the photo-feedback plants, with values of 0.73 and 0.66 respectively by the end of the photoperiod. Meanwhile,  $Fv'/Fm'$  in the controlled treatment exhibited a decline later in the photoperiod. In contrast, after a parallel early decline in the feedback condition, the system maintained a steady maximal quantum efficiency for the larger part of the day. Overall, the photo-feedback system reduced the total light input by  $2.78 \text{ mol m}^{-2} \text{ d}^{-1}$  compared to the control ( $p < 0.01$ ), saving 11.2 % photons, along with the positive impact on growth (Fig. 4 & 5).

To gain a better understanding of the magnitude of the observed differences, Cohen's  $d$  effect sizes were calculated for all yield and energy data reported here (Fig. 9). The absolute value indicates the importance of the results, and standard descriptors (negligible (0 to 0.2), small (0.2 to 0.5), medium (0.5 to 0.8) and large ( $>0.8$ )) were applied. Mass and leaf area yield increases ranged from *small* to *large* effect sizes. The value for fresh mass, dry mass and leaf area were 0.40, 0.62 and 0.85 respectively. However, when normalised for energy use, effect sizes increased to *medium* or *large* reflecting the impact of the combination of yield and energy use. The effect size for energy use was 1.08, while fresh mass ( $\text{g kWh}^{-1}$ ) was 0.61, dry mass ( $\text{g kWh}^{-1}$ ) was 1.17 and 0.98 for leaf area ( $\text{cm}^2 / \text{kWh}^{-1}$ ). In contrast, the non-significant results for relative water content (RWC) and specific leaf area (SLA) were matched by effect sizes of 0.08 and 0.26 respectively.

#### 4. Discussion

In CEA, one of the greatest challenges is the high energy cost of operating LED lighting [18]. Advances in LED technology and improvements in light recipes mitigate costs to some extent [11,22–24,27,51], although current approaches have yet to fully realise the capabilities and flexibilities of modern lighting systems. This lack of exploitation of LED technology has slowed progress towards net zero emission targets in CEA including VFs [18]. Here we demonstrate the potential of a photo-physiological feedback system that utilizes real time plant measurements of photosynthetic efficiency to determine growth light intensity based on plant demands. This not only optimized photosynthetic performance in the crop but also reduced energy consumption with potentially substantial financial savings and a reduced carbon footprint.

Crop productivity is a function of accumulated photosynthetic primary productivity, which is dependent on light intensity and day length. Under long-day lighting conditions ( $> 6 \text{ h}$ ), there is a progressive loss of photosynthetic carbon gain towards the latter part of the diurnal period [29] (Fig. 1). This phenomenon has been demonstrated in both field, under dynamic fluctuating conditions and even in controlled

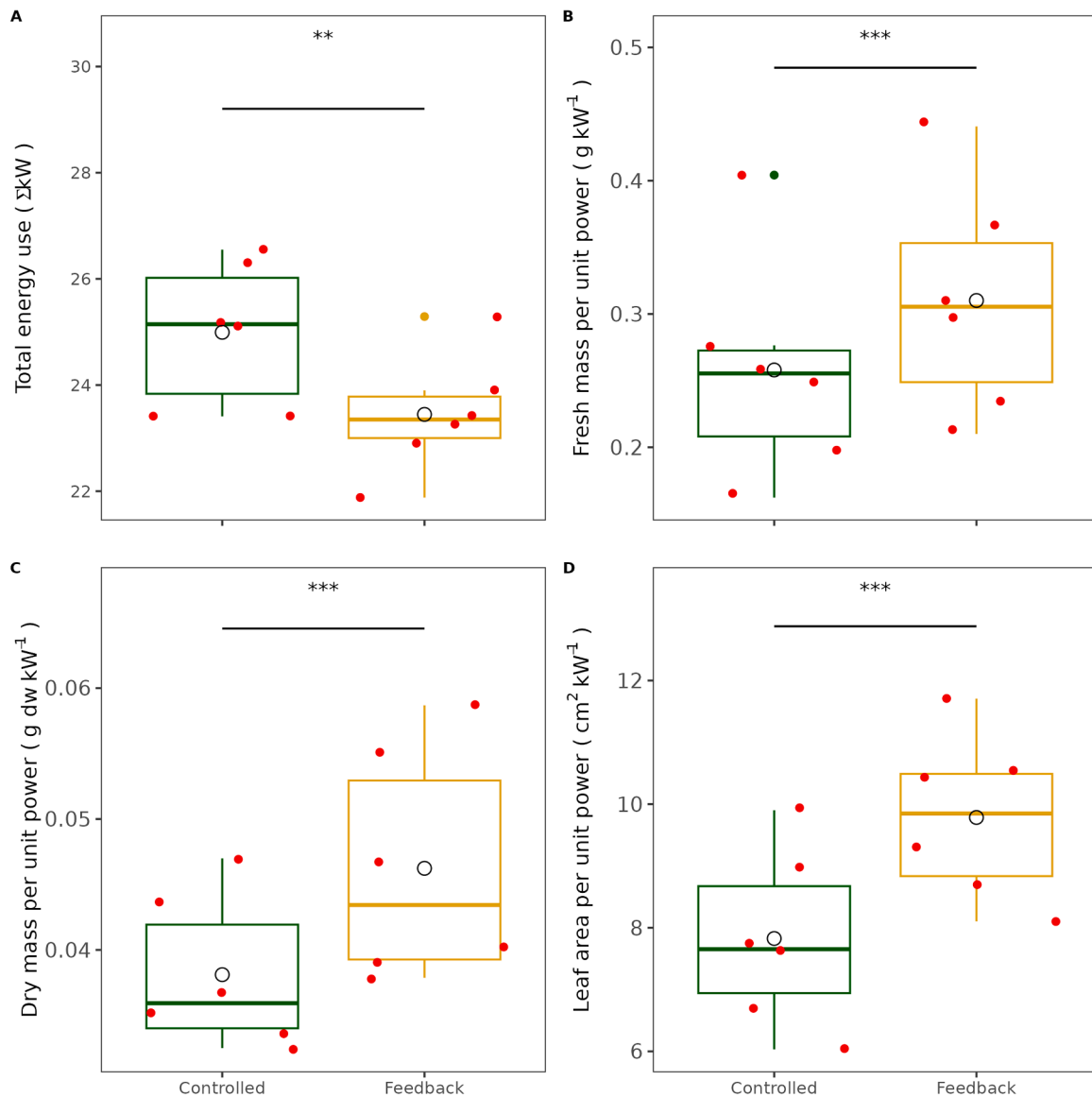


**Fig. 5. Energy used relative to biomass.** Power use was reduced in the feedback condition. A) Total power use in each experiment was significantly lower in the feedback condition. B) Fresh mass achieved  $kWh^{-1}$  was significantly higher in the feedback condition, as was C) dry mass  $kWh^{-1}$  and D) leaf area  $kWh^{-1}$ . Red points represent the means of 12 technical replicates for each independent trial, and the black circle is the overall mean for each treatment,  $n = 6$ . Significance levels: \*\*\* = 0.001, \*\* = 0.01, \* = 0.05.

environments under constant square-wave light regimes [29,49] (Fig. 1). The decline in assimilation rate has been attributed to the accumulation of photosynthate [52] or limited sink capacity [32,53] resulting in negative feedback on the Calvin cycle via changes in photosynthetic gene expression [53,54] and/or an increase in apoplastic sucrose near the stomata due to the rate of transpiration [55–59]. The observed parallel decrease in  $Fq'/Fm'$  and  $Fq'/Fv'$  (Figs. 7B& 8) along with the drop in A (Fig. 7A) support the idea of a reduction in Calvin cycle activity that results in a decreased sink capacity for the end products of electron transport [29,30,32]. The fact that little change was observed in  $Fv'/Fm'$  (Fig. 8) indicates that there was little change in non-photochemical processes [30,32]. Although light is a key driver of photosynthesis, too high a light intensity is either wasted (and dissipated as heat through NPQ processes) or can result in damage to the photosystems lowering overall plant performance [60,61], which can be cumulative and lead to longer lasting decreases in efficiency [32]. Here plants grown using the feedback system consistently showed greater photochemical quenching ( $Fq'/Fv'$ ) in the later part of the photoperiod (Fig. 8), indicating that the plant is using the light energy more

efficiently for carbon fixation and reducing the requirement to waste energy as heat.

The decrease in A over the photoperiod in square wave control conditions resulted in a 28.8 % (Fig. 1) reduction in potential carbon assimilation, which could have major implications for crop growth. Recent studies focusing on improving crop productivity using transgenic approaches to manipulating key genes in photosynthesis have shown substantial yield increases with more modest gains in photosynthesis of ca. 5–10 % [62,63]. The improvements in photosynthetic efficiency over the course of the day achieved using our photo-feedback system, resulted in similarly enhanced crop growth and higher biomass as gains made by transgenic approaches.

Important economic indicators of crop performance in the leafy green sector, include fresh weight (and sometimes leaf area) with commercial products typically sold by weight as bagged salad. Here we measured both fresh and dry biomass as well as leaf area and demonstrated that the increase in biomass was due to greater plant growth and not increased water content. This is important as a high-water content can dilute flavour and affect shelf life and crop quality [64,65].

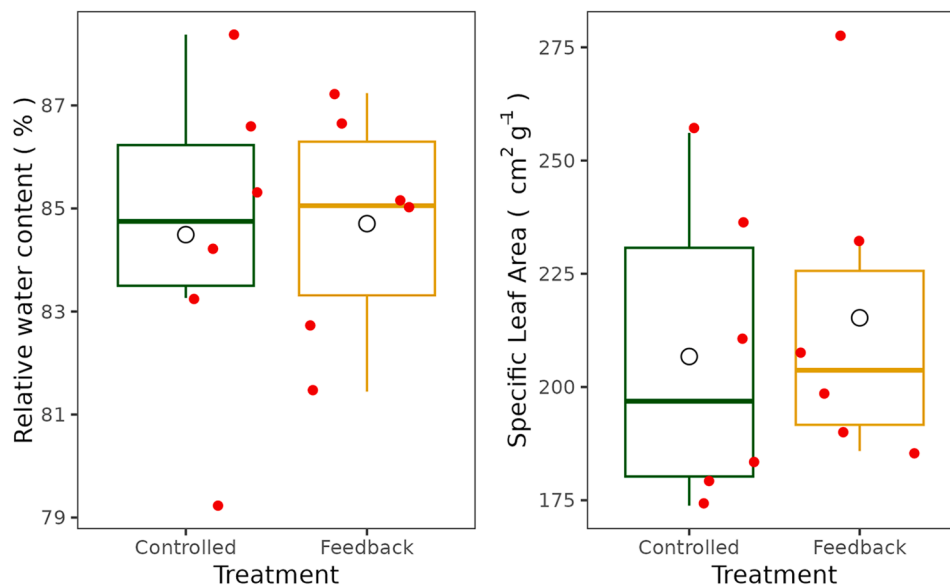


**Fig. 6. Relative water content and specific leaf area.** No differences in key measures of plant physiology were observed, despite the higher harvests for the feedback treatment (see Fig. 4, main text). Data were analysed using a linear mixed effects model of the form  $\text{lme}(\text{Harvest} \sim \text{Treatment} + (1|\text{Experiment\_number}))$ . This approach captured more of the uncertainty in the (semi-controlled) environmental conditions experienced compared to a traditional linear model. Aikike Information Criteria were consistent for all results, with the mixed-effects model outperforming the linear model. A. Relative water content was the same ( $p = 0.71$ ) for both controlled and feedback regimes, B. Specific leaf area (a proxy for leaf thickness) was also the same between treatments ( $p = 0.24$ ). Red points represent the means of 12 technical replicates for each independent trial, and the black circle is the overall mean for each treatment,  $n = 6$ .

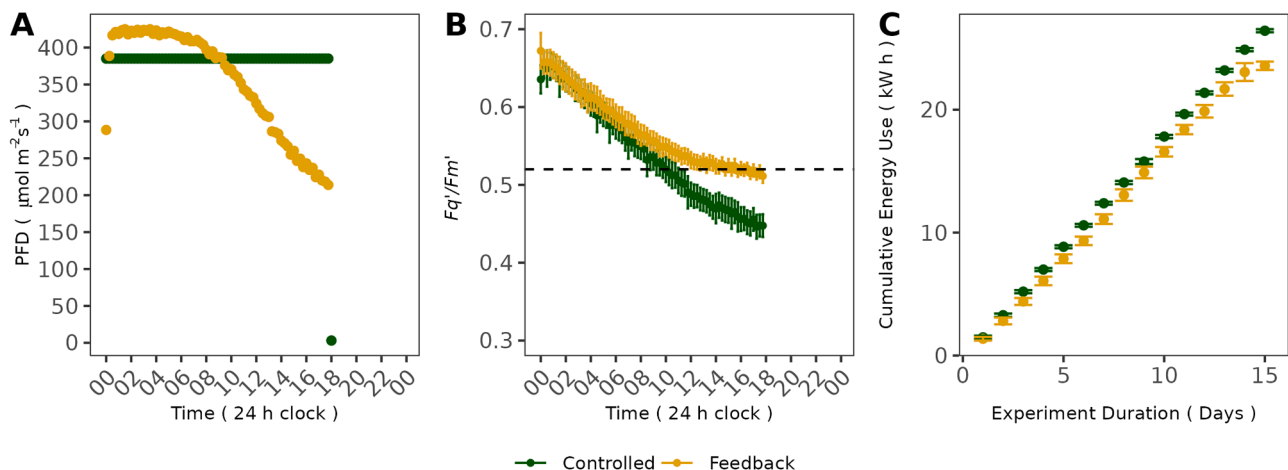


**Fig. 7. PFD and photosynthetic efficiency over the diurnal period.** Comparison of light intensity demand and chlorophyll fluorescence between a controlled, constant light setting (green) and the feedback condition of variable light setting (golden brown) for basil plants. A) While the light intensity delivered in the controlled condition was fixed at  $385 \mu\text{mol m}^{-2} \text{s}^{-1}$  for 18 h and zero for the rest of the 24 h day, in the feedback condition, light intensity was allowed to vary between 100 and  $450 \mu\text{mol m}^{-2} \text{s}^{-1}$  based on the functioning of the feedback loop with constants used as determined in Fig. 3, with a mean value of  $342 \mu\text{mol m}^{-2} \text{s}^{-1}$ . A general pattern was established in the feedback case of higher demand than the controlled condition in the first  $\sim 9$  h of the day, with falling demand below that of the controlled condition in the second half of the photoperiod. Means shown  $\pm$  SE,  $n = 6$ . B). No differences between treatments were observed in  $Fq'/Fm'$  for the first  $\sim 9$  h of the day (The feedback condition was limited to  $450 \mu\text{mol m}^{-2} \text{s}^{-1}$  PFD, preventing the value of  $Fq'/Fm'$  being forced down to the setpoint by higher light intensity). Thereafter  $Fq'/Fm'$  observed in the feedback condition were consistently higher than those observed for the controlled condition, and they remained close to the setpoint for the remainder of the photoperiod. During this second phase, the minimum value of PFD of  $100 \mu\text{mol m}^{-2} \text{s}^{-1}$  and limit the integral error (integral wind-up) in the first period prevented the system from continually hitting the setpoint. C. Cumulative energy demand was consistently lower in the feedback condition compared to the controlled condition. Means shown  $\pm$  SE,  $n = 6$ .

The lowering of light intensity towards the latter half of the diel period by the photo-feedback system greatly reduced energy use, with substantial cost and carbon savings. Importantly the greater biomass along with the decrease in energy input significantly increased all yield measures per unit power (Fig. 5), demonstrating the great potential of optimizing LED inputs based on biological demand to enhance overall crop performance.

Potentially, the interaction between yield and energy use is

important as growers can choose which combination of strategic outcomes they prefer. Control parameters such as the  $Fq'/Fm'$  setpoint, maximum / minimum PFD values, and control loop constants can be manipulated to prioritise any combination of yield and energy use. For example, targeting a lower  $Fq'/Fm'$  while increasing maximum allowable PFD when energy prices are low could deliver higher yield and shorter cycles for a constant carbon footprint. Alternatively, by increasing the  $Fq'/Fm'$  setpoint, yield could be maintained in longer



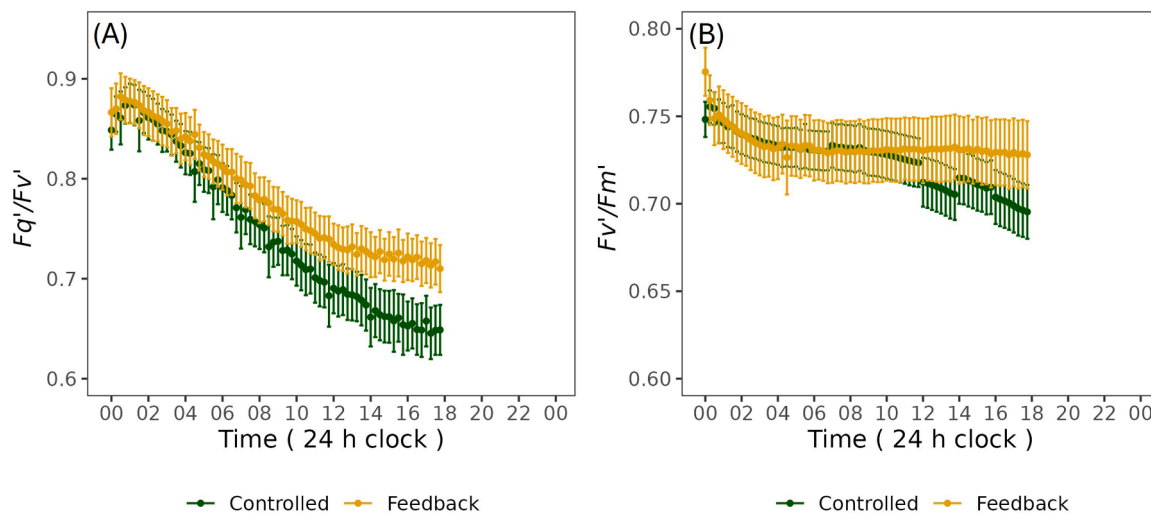


**Fig. 8. Breakdown of chlorophyll fluorescence parameters.** (a) The number of open reaction centres (estimated as  $Fq'/Fv'$  using chlorophyll fluorescence). Under an 18 h photoperiod, with the controlled condition being at  $385 \mu\text{mol m}^{-2} \text{s}^{-1}$  and the feedback treatment receiving a variable PFD between  $450$  and  $100 \mu\text{mol m}^{-2} \text{s}^{-1}$ . (B) The maximum quantum efficiency of PSII as determined by chlorophyll fluorescence under controlled and feedback treatments. Under the controlled condition, PFD was maintained at  $385 \mu\text{mol m}^{-2} \text{s}^{-1}$ . Means shown  $\pm$  SE,  $n = 6$ .

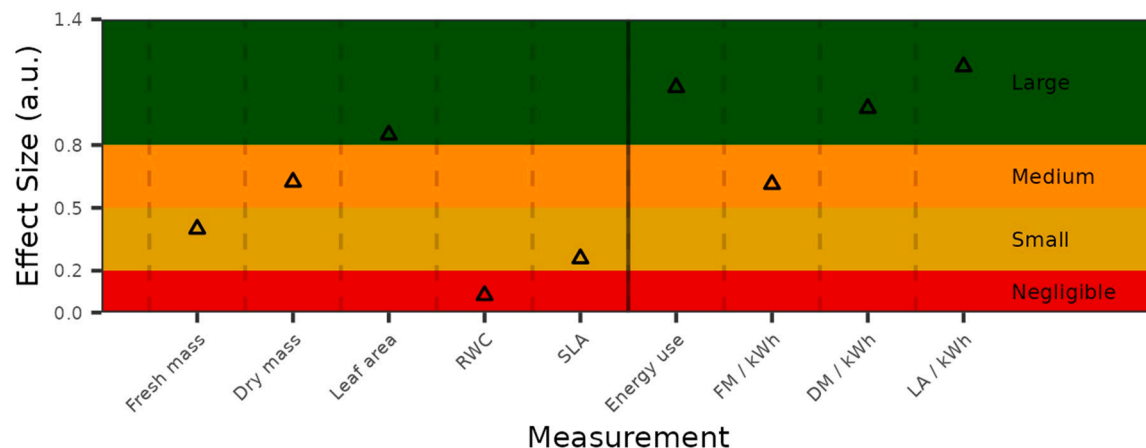


**Fig. 9. The effect size (Cohen's  $d$ )** was calculated for key yield and power consumption results (see Figs. 4, 5, & 6). The magnitude of the effect was *large* for: leaf area, energy use, dry mass  $\text{kWh}^{-1}$ , and leaf area  $\text{kWh}^{-1}$ . The combination of power and yield elements improved the observed effect sizes, ( $n = 6$ ).

cycles with lower energy input and a reduced carbon footprint. A further capability of the system is flexibility within cycles to adjust harvest timing dependent on the growers' or buyers' requirements. Crucially, the observed increases in biomass were as a consequence of photosynthetic carbon accumulation as opposed to higher leaf water content, implying no change in crop quality despite the lower energy requirement. In addition, leaves were no thinner even though leaf area was increased, accelerating carbon capture the longer a crop stays on the system. This may prove to be important for crops with long dwell times in CEA systems such as strawberries or tomatoes.

The work covered in this paper targets outcomes based on continuous dynamic control of light intensity, yet any perturbations in plant metabolism will directly impact  $Fq'/Fm'$  [30]. Therefore, the methods outlined here can provide a sensitive indicator of plant health and stress. Photo-feedback could be used to control temperature, VPD, and water or nutrient availability in the same way as light to optimise inputs relative to outputs and therefore maximize sustainability. Although physiological changes resulting from varying these environmental parameters often emerge over timescales longer than near-instantaneous light responses, the applicability of our approach remains. Yields are driven by both abiotic (environmental) factors as well as biotic challenges. An

additional use for our photo-feedback system is early warning of declining crop health, including, for example, disease [34,66,67]. Interventions could include application of specific spectra such as UV, or reduction in relative humidity / temperature to manage the spread of pathogens [68,69]. Extending the control function to the broader suite of chlorophyll fluorescence signals beyond  $Fq'/Fm'$  could unlock additional applications. Using environmental measurements as inputs to a machine learning algorithm could predict the pathway to deliver fluorescence-based control solutions. Simultaneous adjustment of environmental inputs would provide the minimum-energy solution that maximises performance, yield and sustainability.

While this work considered *O. basilicum*, similar patterns of diurnal photosynthetic responses have been reported for other species [27,49,50]. As chlorophyll fluorescence is a universal indicator of performance across all photosynthetic organisms, we expect this technology to be applicable to many crops, such as other leafy greens or perennials grown under either supplemental or totally artificially lit growing environments [32]. The photo-feedback technology can be applied across any agricultural system where input(s) can be manipulated. Those inputs could range from pesticide application through environmental control, to cultivar selection. A key feature of the system is that the technology is

inexpensive, physically robust, scientifically established, and easy to use for the non-specialist. Given the variability of environmental conditions within our study (for example, our observed temperatures ranged from 35.5 °C down to 18.5 °C against a setpoint of 23 °C (Supp. Table 1)), we believe the photo-feedback system would continue to work in less-controlled environments such as glasshouses and large vertical farms. Here we have demonstrated the potential commercial benefits of our real time biological feedback system, with considerable energy (cost) savings alongside enhanced biomass. However, a full cost benefit analyses would be required to evaluate the commercial return of investment on implementation at large scale. It is worth noting that fluorimeters are becoming increasingly developed and available for commercial agronomic markets and for a fraction of the price of the research instrument used here.

Use of the feedback system in this study decreased carbon emissions per FW yield, by 17.3 % (suppl. Data 1). However, in absolute carbon accounting, our study was far less efficient than large scale vertical farms. Martin et al. (2023) [70] reported an expected 0.98 g CO<sub>2</sub> emitted per g FW yield, whereas our control and feedback systems were an order of magnitude larger. This large discrepancy in efficiency is due to multiple factors. Firstly, the LED luminaires (Dyna, Heliospectra) used in our study are designed for research purposes and therefore their efficacy is far lower than lighting purely designed for crop growth within a vertical farm. Secondly, experiments were conducted under small spatial scales, each treatment requiring a dedicated luminaire, and in contrast, a commercial vertical farm would grow hundreds of plants under a lighting array of similar capacity to the one used here. Our study was designed to demonstrate potential energy savings and yield enhancement, through matching biological diel demand (based on photosynthetic efficiency) with light intensity, and comparing the relative differences with standard square constant light regimes.

In conclusion we have demonstrated that our integrated, 'intelligent' systems approach can interpret real-time plant signals by combining the latest physiological tools, modern LED technology and knowledge of plant primary metabolism to deliver adaptable and optimised lighting recipes determined by crop demand. Our strategy substantially improved crop yield by 13.5 %, lowered the carbon footprint by 17 %, and reduced energy consumption by 6.2 %. Our approach directly addresses current global challenges in food security, net zero and environmental sustainability.

## Ethical statement

The authors have followed ethical guidelines.

## Data statement

Data are available at <https://researchdata.essex.ac.uk/234> / (DOI - <https://doi.org/10.5526/erdr-00000234>).

## CRedit authorship contribution statement

**Jim Stevens:** Writing – review & editing, Writing – original draft, Methodology, Investigation, Formal analysis, Data curation. **Phillip Davey:** Writing – review & editing, Writing – original draft, Investigation, Data curation. **Piotr Kasznicki:** Investigation, Data curation. **Tanja A Hofmann:** Writing – review & editing. **Tracy Lawson:** Writing – review & editing, Writing – original draft, Supervision, Resources, Funding acquisition, Conceptualization.

## Declaration of competing interest

The authors declare that they have no known competing financial interests or personal relationships that could have appeared to influence the work reported in this paper.

## Acknowledgements

JS was supported through a EIRA funding to the University of Essex. TL also acknowledges funding support from Leverhulme SF/R1/231041 and BBSRC for the following grant BB/T004274/1; BB/Y001850/1; BB/Y000722/1. We would like to thank Ben Cemlyn for his input on earlier work in this project and thank Shellie Wall for providing the schematic figures.

## Supplementary materials

Supplementary material associated with this article can be found, in the online version, at [doi:10.1016/j.atech.2025.101593](https://doi.org/10.1016/j.atech.2025.101593).

## References

- [1] D. Tilman, C. Balzer, J. Hill, B.L. Befort, Global food demand and the sustainable intensification of agriculture, *Proc. Natl. Acad. Sci.* 108 (2011) 20260–20264, <https://doi.org/10.1073/pnas.1116437108>.
- [2] J.A. Foley, Can we feed the world sustain the planet? *Sci. Am.* 305 (2011) 60–65.
- [3] J.A. Foley, N. Ramankutty, K.A. Brauman, E.S. Cassidy, J.S. Gerber, M. Johnston, N.D. Mueller, C. O'Connell, D.K. Ray, P.C. West, C. Balzer, E.M. Bennett, S. R. Carpenter, J. Hill, C. Monfreda, S. Polasky, J. Rockström, J. Sheehan, S. Siebert, D. Tilman, D.P.M. Zaks, Solutions for a cultivated planet, *Nature* 478 (2011) 337–342, <https://doi.org/10.1038/nature10452>.
- [4] F. Global, Regional and Country trends, 2000–2020, , FAO.[Google Scholar], 2022.
- [5] D.K. Ray, N.D. Mueller, P.C. West, J.A. Foley, Yield trends are insufficient to double global crop production by 2050, *PLoS One* 8 (2013) e66428, <https://doi.org/10.1371/journal.pone.0066428>.
- [6] R. Shamshiri, F. Kalantari, K. Ting, K.R. Thorp, I.A. Hameed, C. Weltzien, D. Ahmad, Z.M. Shad, Advances in greenhouse automation and controlled environment agriculture: a transition to plant factories and urban agriculture, *Int. J. Agric. Biol. Eng.* 11 (2018) 1–22.
- [7] N. Gruda, J. Tanny, Protected crops, in: *Horticulture: Plants for People and Places, Volume 1: Production Horticulture*, Springer, 2014, pp. 327–405.
- [8] N.H. Doddrell, T. Lawson, C.A. Raines, C. Wagstaff, A.J. Simkin, Feeding the world: impacts of elevated [CO<sub>2</sub>] on nutrient content of greenhouse grown fruit crops and options for future yield gains, *Hortic. Res.* 10 (2023), <https://doi.org/10.1093/hr/uhad026>.
- [9] T. Van Gerrewy, N. Boon, D. Geelen, Vertical farming: the only way is up? *Agronomy* 12 (2021) 2.
- [10] M.W. van Iersel, D. Gianino, An adaptive control approach for light-emitting diode lights can reduce the energy costs of supplemental lighting in greenhouses, *HortScience* 52 (2017) 72–77.
- [11] J.D. Stamford, J. Stevens, P.M. Mullineaux, T. Lawson, LED lighting: a grower's guide to light spectra, *HortScience* 58 (2023) 180–196.
- [12] C. Wong, J. Wood, S. Paturi, Vertical farming: an assessment of Singapore City, *Eotrop. Electron. J. Stud. Trop.* 19 (2020) 228–248.
- [13] S. Van Delden, M. SharathKumar, M. Butturini, L. Graamans, E. Heuvelink, M. Kacira, E. Kaiser, R. Klamer, L. Klerkx, G. Kootstra, Current status and future challenges in implementing and upscaling vertical farming systems, *Nat. Food* 2 (2021) 944–956.
- [14] A.M. Beacham, L.H. Vickers, J.M. Monaghan, Vertical farming: a summary of approaches to growing skywards, *J. Hortic. Sci. Biotechnol.* 94 (2019) 277–283, <https://doi.org/10.1080/14620316.2019.1574214>.
- [15] Z. Bian, N. Jiang, S. Grundy, C. Lu, Uncovering LED light effects on plant growth: new angles and perspectives - LED light for improving plant growth, nutrition and energy-use efficiency. *Acta Horticulturae*, International Society for Horticultural Science (ISHS), Leuven, Belgium, 2018, pp. 491–498, <https://doi.org/10.17660/ActaHortic.2018.1227.62>.
- [16] M.J. Abdullah, Z. Zhang, K. Matsubae, Potential for food self-sufficiency improvements through indoor and vertical farming in the Gulf Cooperation Council: challenges and opportunities from the case of Kuwait, *Sustainability* 13 (2021) 12553, <https://doi.org/10.3390/su132212553>.
- [17] L. Graamans, A. van den Dobbelsteen, E. Meinen, C. Stanghellini, Plant factories: crop transpiration and energy balance, *Agric. Syst.* 153 (2017) 138–147, <https://doi.org/10.1016/j.agsy.2017.01.003>.
- [18] C. Stanghellini, D. Katzin, The dark side of lighting: a critical analysis of vertical farms' environmental impact, *J. Clean. Prod.* 458 (2024) 142359.
- [19] L. Casey, B. Freeman, K. Francis, G. Brychkova, P. McKeown, C. Spillane, A. Bezrukov, M. Zaworotko, D. Styles, Comparative environmental footprints of lettuce supplied by hydroponic controlled-environment agriculture and field-based supply chains, *J. Clean. Prod.* 369 (2022) 133214, <https://doi.org/10.1016/j.jclepro.2022.133214>.
- [20] N. Cowan, L. Ferrier, B. Spears, J. Drewer, D. Reay, U. Skiba, CEA systems: the means to achieve future food security and environmental sustainability? *Front. Sustain. Food Syst.* 6 (2022) <https://doi.org/10.3389/fsufs.2022.891256>.
- [21] S. Palmer, M.W. van Iersel, Increasing growth of lettuce and mizuna under sole-source LED lighting using longer photoperiods with the same daily light integral, *Agronomy* 10 (2020) 1659.

- [22] J.A. Nelson, B. Bugbee, Economic analysis of greenhouse lighting: light emitting diodes vs. high intensity discharge fixtures, *PLoS One* 9 (2014) e99010.
- [23] B. Bugbee, Economics of LED lighting. *Light Emitting Diodes For Agriculture: Smart Lighting*, Springer, 2017, pp. 81–99.
- [24] M.W. van Iersel, Optimizing LED lighting in controlled environment agriculture. *Light Emitting Diodes For Agriculture: Smart Lighting*, Springer, 2017, pp. 59–80.
- [25] C. Miao, S. Yang, J. Xu, H. Wang, Y. Zhang, J. Cui, H. Zhang, H. Jin, P. Lu, L. He, Effects of light intensity on growth and quality of lettuce and spinach cultivars in a plant factory, *Plants* 12 (2023) 3337.
- [26] F.A. Busch, E.A. Ainsworth, A. Amtmann, A.P. Cavanagh, S.M. Drierer, J. N. Ferguson, J. Kromdijk, T. Lawson, A.D.B. Leakey, J.S.A. Matthews, K. Meacham-Hensold, R.L. Vath, S. Violet-Chabrand, B.J. Walker, M. Papanatsiou, A guide to photosynthetic gas exchange measurements: fundamental principles, best practice and potential pitfalls, *Plant Cell Env.* 47 (2024) 3344–3364, <https://doi.org/10.1111/pce.14815>.
- [27] J.D. Stamford, T.A. Hofmann, T. Lawson, Sinusoidal LED light recipes can improve rocket edible biomass and reduce electricity costs in indoor growth environments, *Front. Plant Sci.* 15 (2024) 1447368.
- [28] J.S.A. Matthews, S.R.M. Violet-Chabrand, T. Lawson, Diurnal variation in gas exchange: the balance between carbon fixation and water loss, *Plant Physiol.* 174 (2017) 614–623, <https://doi.org/10.1104/pp.17.00152>.
- [29] S. Violet-Chabrand, J.S. Matthews, A.J. Simkin, C.A. Raines, T. Lawson, Importance of fluctuations in light on plant photosynthetic acclimation, *Plant Physiol.* 173 (2017) 2163–2179.
- [30] N.R. Baker, Chlorophyll fluorescence: a probe of photosynthesis In Vivo, *Annu. Rev. Plant Biol.* 59 (2008) 89–113, <https://doi.org/10.1146/annurev.arplant.59.032607.092759>.
- [31] M. Ludwig, J. Hartwell, C.A. Raines, A.J. Simkin, The Calvin-Benson-Bassham cycle in C4 and Crassulacean acid Metabolism Species, Elsevier, 2024, pp. 10–22.
- [32] E.H. Murchie, T. Lawson, Chlorophyll fluorescence analysis: a guide to good practice and understanding some new applications, *J. Exp. Bot.* 64 (2013) 3983–3998, <https://doi.org/10.1093/jxb/ert208>.
- [33] J. Cavender-Bares, F.A. Bazzaz, From leaves to ecosystems: using chlorophyll fluorescence to assess photosynthesis and plant function in ecological studies, in: G. C. Papageorgiou, Govindjee (Eds.), *Chlorophyll a Fluorescence: A Signature of Photosynthesis*, Springer Netherlands, Dordrecht, 2004, pp. 737–755, [https://doi.org/10.1007/978-1-4020-3218-9\\_29](https://doi.org/10.1007/978-1-4020-3218-9_29).
- [34] E. Gorbe, A. Calatayud, Applications of chlorophyll fluorescence imaging technique in horticultural research: a review, *Sci. Hortic.* 138 (2012) 24–35, <https://doi.org/10.1016/j.scienta.2012.02.002>.
- [35] C. Elkins, M.W. van Iersel, Longer photoperiods with the same daily light integral increase daily electron transport through photosystem II in Lettuce, *Plants* 9 (2020) 1172, <https://doi.org/10.3390/plants9091172>.
- [36] C. Elkins, M.W. van Iersel, Longer photoperiods with the same daily light integral improve growth of rudbeckia seedlings in a greenhouse, *HortScience* 55 (2020) 1676–1682.
- [37] G. Weaver, M.W. van Iersel, Longer photoperiods with adaptive lighting control can improve growth of greenhouse-grown 'Little Gem' lettuce (*Lactuca sativa*), *HortScience* 55 (2020) 573–580.
- [38] T. Pocock, Light-emitting diodes and the modulation of specialty crops: light sensing and signaling networks in plants, *HortScience* 50 (2015) 1281–1284, <https://doi.org/10.21273/HORTSCI.50.9.1281>.
- [39] N.R. Baker, E. Rosenqvist, Applications of chlorophyll fluorescence can improve crop production strategies: an examination of future possibilities, *J. Exp. Bot.* 55 (2004) 1607–1621, <https://doi.org/10.1093/jxb/erh196>.
- [40] G. Lauria, C. Ceccanti, E. Lo Piccolo, H. El Horri, L. Guidi, T. Lawson, M. Landi, "Metabolight": how light spectra shape plant growth, development and metabolism, *Physiol. Plant* 176 (2024) e14587.
- [41] M. Van Iersel, E. Mattos, G. Weaver, R. Ferrarezi, M. Martin, M. Haidekker, Using chlorophyll fluorescence to control lighting in controlled environment agriculture, in: 2016: pp. 427–434.
- [42] M.W. van Iersel, G. Weaver, M.T. Martin, R.S. Ferrarezi, E. Mattos, M. Haidekker, A chlorophyll fluorescence-based biofeedback system to control photosynthetic lighting in controlled environment agriculture, *J. Am. Soc. Hortic. Sci.* 141 (2016) 169–176.
- [43] W. Jin, D. Formiga Lopez, E. Heuvelink, L.F. Marcelis, Light use efficiency of lettuce cultivation in vertical farms compared with greenhouse and field, *Food Energy Secur.* 12 (1) (2023) e391.
- [44] Rs. Team, RStudio: integrated development for R, RStudio Inc. Boston MA 700 (2015) 879.
- [45] R Core Team, R: A language and Environment For Statistical Computing, R Foundation for Statistical Computing, Vienna, Austria, 2016. <http://www.R-project.org/>.
- [46] D. Bates, M. Mächler, B. Bolker, S. Walker, Fitting linear mixed-effects models using lme4, *J. Stat. Softw.* 67 (2015) 1–48, <https://doi.org/10.18637/jss.v067.i01>.
- [47] J. Fox, S. Weisberg, *An R Companion to Applied Regression*, SAGE Publications, 2018.
- [48] J. Cohen, *Statistical Power Analysis For the Behavioral Sciences*, 2nd ed., Routledge, New York, 2013 <https://doi.org/10.4324/9780203771587>.
- [49] J.S. Matthews, S. Violet-Chabrand, T. Lawson, Acclimation to fluctuating light impacts the rapidity of response and diurnal rhythm of stomatal conductance, *Plant Physiol.* 176 (2018) 1939–1951.
- [50] W. Suwannarat, S. Violet-Chabrand, E. Kaiser, Diurnal decline in photosynthesis and stomatal conductance in several tropical species, *Front. Plant Sci.* 14 (2023) 1273802.
- [51] P. Kusuma, P.M. Pattison, B. Bugbee, From physics to fixtures to food: current and potential LED efficacy, *Hortic. Res.* 7 (2020).
- [52] M. Stitt, Rising CO2 levels and their potential significance for carbon flow in photosynthetic cells, *Plant Cell Env.* 14 (1991) 741–762.
- [53] M.J. Paul, C.H. Foyer, Sink regulation of photosynthesis, *J. Exp. Bot.* 52 (2001) 1383–1400.
- [54] M.J. Paul, T.K. Pellny, Carbon metabolite feedback regulation of leaf photosynthesis and development, *J. Exp. Bot.* 54 (2003) 539–547.
- [55] P. Lu, S.Q. Zhang, W.H. Outlaw, K.A. Riddle, Sucrose: a solute that accumulates in the guard-cell apoplast and guard-cell symplast of open stomata, *FEBS Lett.* 362 (1995) 180–184.
- [56] J. Outlaw, H. William, Integration of cellular and physiological functions of guard cells, *CRC. Crit. Rev. Plant Sci.* 22 (2003) 503–529.
- [57] Y. Kang, W.H. Outlaw, P.C. Andersen, G.B. Fiore, Guard-cell apoplastic sucrose concentration—a link between leaf photosynthesis and stomatal aperture size in the apoplastic phloem loader *Vicia faba* L, *Plant Cell Env.* 30 (2007) 551–558.
- [58] G. Kelly, M. Moshelion, R. David-Schwartz, O. Halperin, R. Wallach, Z. Attia, E. Belausov, D. Granot, Hexokinase mediates stomatal closure, *Plant J.* 75 (2013) 977–988.
- [59] T. Lawson, A.J. Simkin, G. Kelly, D. Granot, Mesophyll photosynthesis and guard cell metabolism impacts on stomatal behaviour, *New. Phytol.* 203 (2014) 1064–1081.
- [60] S.B. Powles, Photoinhibition of photosynthesis induced by visible light, *Annu Rev. Plant Physiol.* 35 (1984) 15–44.
- [61] J.A. Raven, The cost of photoinhibition, *Physiol. Plant* 142 (2011) 87–104.
- [62] A.J. Simkin, P.E. López-Calcano, C.A. Raines, Feeding the world: improving photosynthetic efficiency for sustainable crop production, *J. Exp. Bot.* 70 (2019) 1119–1140, <https://doi.org/10.1093/jxb/ery445>.
- [63] S. Lefebvre, T. Lawson, M. Fryer, O.V. Zakhleniuk, J.C. Lloyd, C.A. Raines, Increased sedoheptulose-1,7-bisphosphatase activity in transgenic tobacco plants stimulates photosynthesis and growth from an early stage in development, *Plant Physiol.* 138 (2005) 451–460, <https://doi.org/10.1104/pp.104.055046>.
- [64] M. Agüero, M. Barg, A. Yommi, A. Camelo, S. Roura, Postharvest changes in water status and chlorophyll content of lettuce (*Lactuca sativa* L.) and their relationship with overall visual quality, *J. Food Sci.* 73 (2008) S47–S55.
- [65] J.-S. Lee, D. Chandra, J. Son, Growth, physicochemical, nutritional, and postharvest qualities of leaf lettuce (*Lactuca sativa* L.) as affected by cultivar and amount of applied nutrient solution, *Horticulturae* 8 (2022) 436.
- [66] J.D. Scholes, S.A. Rolfe, Chlorophyll fluorescence imaging as tool for understanding the impact of fungal diseases on plant performance: a phenomics perspective, *Funct. Plant Biol.* 36 (2009) 880–892.
- [67] H. Wang, X. Qian, L. Zhang, S. Xu, H. Li, X. Xia, L. Dai, L. Xu, J. Yu, X. Liu, A method of high throughput monitoring crop physiology using chlorophyll fluorescence and multispectral imaging, *Front. Plant Sci.* 9 (2018) 407.
- [68] Y. Elad, I. Pertot, Climate change impacts on plant pathogens and plant diseases, *J. Crop. Improv.* 28 (2014) 99–139, <https://doi.org/10.1080/15427528.2014.865412>.
- [69] B.A. Kunz, D.M. Cahill, P.G. Mohr, M.J. Osmond, E.J. Vonarx, Plant responses to UV radiation and links to pathogen resistance, *Int. Rev. Cytol.* 255 (2006) 1–40.
- [70] M. Martin, M. Elmour, A.C. Sinol, Environmental life cycle assessment of a large-scale commercial vertical farm, *Sustain. Prod. Consum.* 1 (40) (2023) 182–193.